Molecular Microbiology (2004) **52**(3), 651–660 doi:10.1111/j.1365-2958.2004.03991.x

Solution structure and domain architecture of the divisome protein FtsN

Ji-Chun Yang,[1] Fusinita van den Ent,[1] David Neuhaus,[1] Julian Brevier[2] and Jan Löwe[1]*
[1]*MRC Laboratory of Molecular Biology, Hills Road, Cambridge CB2 2QH, UK.*
[2]*Ecole Normale Supérieure de Lyon, 46, Allée d'Italie, 69364 Lyon Cedex 07, France.*

Summary

Prokaryotic cell division occurs through the formation of a septum, which in *Escherichia coli* requires coordination of the invagination of the inner membrane, biosynthesis of peptidoglycan and constriction of the outer membrane. FtsN is an essential cell division protein and forms part of the divisome, a putative complex of proteins located in the cytoplasmic membrane. Structural analyses of FtsN by nuclear magnetic resonance (NMR) reveals an RNP-like fold at the C-terminus (comprising residues 243–319), which has significant sequence homology to a peptidoglycan-binding domain. Sequential deletion mutagenesis in combination with NMR shows that the remaining of the periplasmic region of FtsN is unfolded, with the exception of three short, only partially formed helices following the *trans*-membrane helix. Based on these findings we propose a model in which FtsN, anchored in the inner membrane, bridges over to the peptidoglycan layer, thereby enabling the coordination of the divisome and the murein-shaping machinery in the periplasm.

Introduction

Correct cell division in *Escherichia coli* is initiated by formation of the septum at mid-cell, which constricts the cytoplasmic (inner) membrane. Synthesis of the septal peptidoglycan layer and invagination of the outer membrane complete this process, separating the two daughter cells. The first indication of septum formation is a ring-like structure at mid-cell formed by FtsZ, the bacterial tubulin homologue, which forms the heart of the divisome (septal ring). Once FtsZ is located at mid-cell, other components of the division machinery are recruited. The order of appearance of the divisome components was genetically determined and comprises FtsA/ZipA, FtsK, FtsQ, FtsL/YgbQ, FtsW, FtsI (PBP3), FtsN and *N*-acetylmuramoyl-L-alanine amidase AmiC (reviewed in refs Lutkenhaus and Addinall, 1997; Rothfield *et al*., 1999; Errington *et al*., 2003). The exact function of the majority of the divisome components are unknown. FtsZ and FtsA reside in the cytoplasm, whereas FtsQ, FtsI, FtsL/YgbQ and FtsN each have an N-terminal transmembrane-spanning helix. FtsK and FtsW bridge the membrane several times. Only recently the first entirely periplasmic component of the divisome was identified, AmiC (Bernhardt and de Boer, 2003). One possible model for invagination of the septum is that the constriction of the cytoplasmic membrane is driven by the FtsZ ring and the associated divisome, with its anchor in the inner membrane. In order to shape the newly formed polar caps, murein needs to be synthesized and the old cell wall cross-links need to be destroyed (Vollmer and Holtje, 2001). At present the only known component of the divisome associated with the highly specific peptidoglycan synthesis machinery is the DD-transpeptidase FtsI (PBP3) (Ishino and Matsuhashi, 1981; Adam *et al*., 1997). The periplasmic murein hydrolases (AmiA, AmiB and AmiC) are responsible for degradation of murein, cleaving the bond between the peptide and the *N*-acetylmuramic acid. In the absence of these amidases, long chains of non-separating cells build up, indicating that the amidases play a role in the final stages of division (Heidrich *et al*., 2001; 2002). Recently, AmiC was shown to localize to the division site in a FtsN-dependent manner (Bernhardt and de Boer, 2003). However, a direct interaction between FtsN and AmiC has not been identified.

The requirement of FtsN for cell division in *E. coli* became obvious with a conditional null allele of the *ftsN* gene that results in long, filamentous cells that eventually die. FtsN was identified as a multicopy suppressor of a temperature sensitive *ftsA* mutant (*ftsA12*) and also acted as a suppressor of the temperature sensitive mutants *ftsI23*, *ftsQ1*, *ftsk44 and ftsk3531* but not *ftsZ84* (Dai *et al*., 1993; Draper *et al*., 1998). Septal localization of an FtsN-GFP fusion protein depends on the prior localization or function of FtsZ, FtsA, FtsI and FtsQ and these experiments indicated that the recruitment of FtsN to the septum occurs relatively late (Addinall *et al*., 1997). Although FtsN is essential in *E. coli*, the protein is not widely conserved

Accepted 22 December, 2003. *For correspondence. E-mail jyl@mrc-lmb.cam.ac.uk; Tel. (+44) 1223252969; Fax (+44) 1223213556.

and has clear homologues only in the enteric bacteria and *Haemophilus* spp. (Dai *et al*., 1996). FtsN is a 36 kDa protein and has a simple bitopic topology. A short cytoplasmic domain (residues 1–33) is linked via a membrane-spanning helix (residues 34–53) to the larger C-terminal part (amino acids 54–319) that resides in the periplasm (Addinall *et al*., 1997; Dai *et al*., 1996). Deletion of the cytoplasmic and membrane-spanning domains of FtsN have been shown to cause instability and loss of function. However, the exchange of the *trans*-membrane helix with the membrane-spanning domain of MalG restored the subcellular localization as well as the function of FtsN (Addinall *et al*., 1997). Replacing the *trans*-membrane region of FtsN with the cleavable signal sequence of MalE (Dai *et al*., 1996) produces functional protein as well. Hence, it is the periplasmic domain of FtsN that determines its localization to the division site and contains its essential function. The role of FtsN in cell division is poorly understood. Localization studies suggested that it is assembled late into the divisome, indicating that FtsN could be involved in shaping the murein at the polar caps, as are the late recruits FtsI (murein synthase PBP3) and AmiC (murein hydrolase).

Here we show by sequential deletion mutagenesis in combination with structural analysis of the mutants by NMR that the C-terminal 77 residues form a folded globular domain, which on the sequence level has significant homology to the peptidoglycan-binding domain of an autolysin. Surprisingly, further NMR analyses indicate that the remaining part of the periplasmic domain is unfolded with the exception of three short, only partially folded helices at the N-terminus of the periplasmic domain. Based on these data we propose a model of FtsN function in which it could form a bridge between the cell division machinery located in the cytoplasmic membrane and the peptidoglycan layer in the periplasm.

Results and discussion

NMR analysis of FtsN 58–319

The principal characteristics that allow folded regions of proteins to be distinguished from relatively unstructured (random coil) regions using NMR are the extent of chemical shift dispersion of the signals, the linewidths of the signals and the density of nuclear Overhauser effect (NOE) correlations in a NOE spectroscopy (NOESY) spectrum. For the backbone amide group ^{1}H and ^{15}N signals observed in an heteronuclear single quantum correlation (HSQC) spectrum, the greater chemical shift dispersion characteristic of a folded domain results from a combination of factors, including hydrogen bonding (particularly for the ^{1}H resonances), local backbone geometry, and proximity of magnetically anisotropic groups (especially aromatic rings) and charged groups. In random coil regions, rapid and extensive internal motions largely average these effects away, resulting in a much narrower populated chemical shift range, particularly for the amide group ^{1}H resonances. Linewidths of NMRs are principally determined by the tumbling characteristics (more accurately the rotational correlation time) of the nuclei from which they originate; the slower a group re-orients in solution, the faster will be the NMR relaxation times of nuclei within it and consequently the broader will be the corresponding NMRs. The rapid and extensive internal motions in random coil regions therefore cause groups in these regions to show NMR signals with linewidths quite similar to those for small molecules, whereas linewidths for groups without significant internal motions in structured domains become broader the larger the domain.

In order to assess the likely proportion and approximate location of folded structure in the complete periplasmic domain of FtsN (ECN2 with residues 58–319; Fig. 1), a series of two-dimensional NMR spectra were acquired, including homonuclear total correlation spectroscopy (TOCSY), NOESY and (^{15}N, ^{1}H) HSQC experiments. The TOCSY spectrum of FtsN 58–319 is shown in Fig. 2A, and this gave an early clue that the random coil region of the fragment probably included the N-terminal part. The mixing sequence in a TOCSY experiment (which is the part of the TOCSY pulse sequence responsible for generating the cross peaks) is generally significantly more efficient for narrow resonances than it is for broad ones, with the result that strong cross peaks are seen connecting narrow resonances from within a common spin-system from an unstructured region, whereas cross peaks connecting similarly related but broader resonances from structured domains are often much weaker. Thus the majority of the strong cross peaks seen in Fig. 2A are expected to originate from the random coil portion of the 58–319 fragment. It is noticeable that there are unusually few strong cross peaks linking NH resonances to H^{-} resonances with shifts in the approximate region 2.5–3.5 ppm (indicated by a dashed box in the figure), which for a random coil sequence is the region expected to contain just (NH, H^{-}) cross peaks for most or all of the Asn, Asp, Cys, His, Phe, Trp and Tyr residues (each residue of these types contributes either two such cross peaks aligned at a common NH shift, or else one apparent cross peak in the case that both H^{-} signals are accidentally degenerate). Only seven sets of such strong cross peaks were found, indicating that the random coil region of the 58–319 fragment contains very few of these residue types. Inspection of the sequence (Fig. 1) shows immediately that the C-terminus is relatively rich in these residue types whereas the remainder of the sequence is quite poor.

It is difficult to be strictly quantitative in this analysis, as spectral overlap or rapid solvent exchange of particular

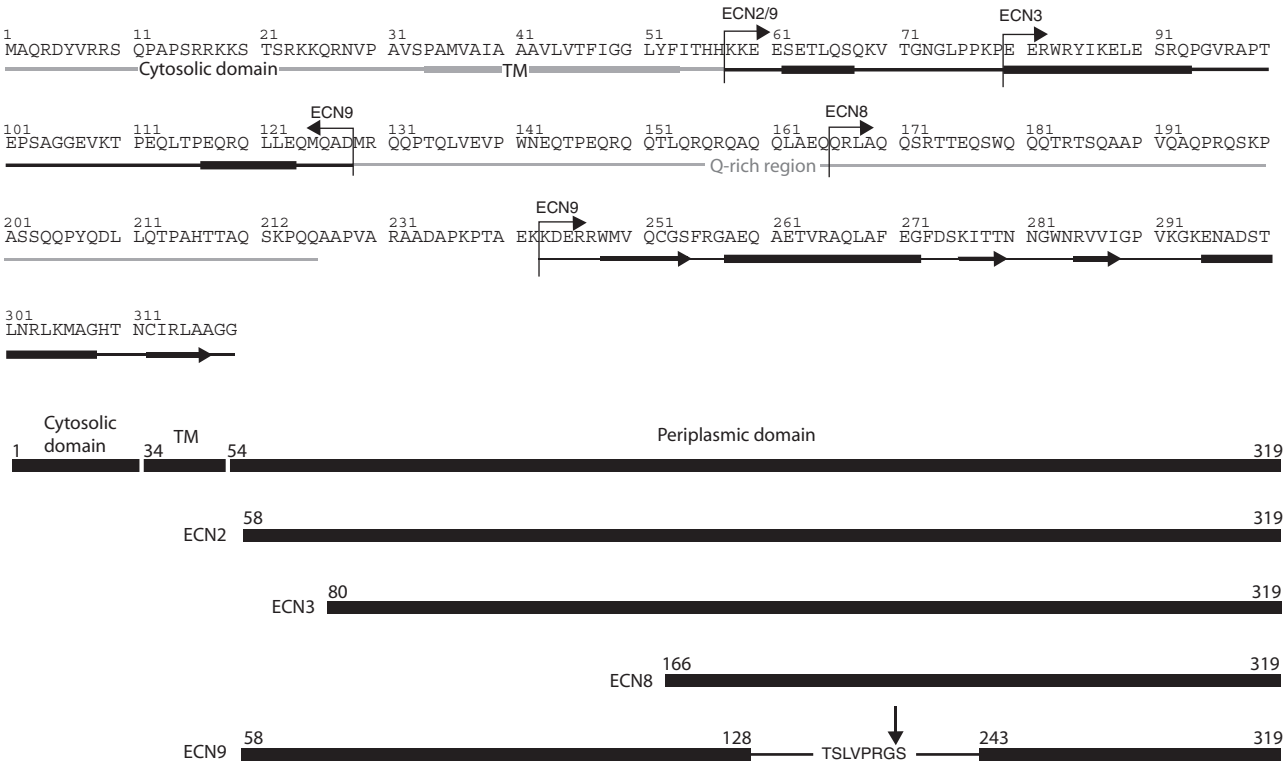

Fig. 1. FtsN constructs. The boundaries of the deletion mutants of FtsN (ECN2, ECN3, ECN8 and ECN9 (N- and C-terminus)) are indicated by the arrows above the FtsN sequence of *E. coli*. The secondary structural elements are depicted below the sequence with an arrow indicating a β-strand and a bar indicating an α-helix. The first three helices in the periplasmic domain are only partially formed and numbers describing the boundaries of these helices are approximate. A schematic representation of FtsN and the deletion mutants in the lower part shows the residue numbers of the termini of the deletion mutants.

amide NH signals may reduce the number of (NH, H) cross peaks actually observed. The HSQC spectrum of FtsN 58–319 shown in Fig. 2B offers further clues as to the proportion of random coil residues present, as the corresponding signals form a characteristic cluster near the centre of the ^{1}H amide chemical shift range (i.e. approximately 8.0–8.5 p.p.m.). Again, truly quantitative analysis is elusive due to extensive overlap amongst the random coil signals, and the expected presence in this region of some signals from the folded region also. Nonetheless, it is quite clear from the combined analysis of the TOCSY and HSQC spectra of FtsN 58–319 that a very significant proportion of this fragment is comprised of random coil residues, and that the random coil region does not include the C-terminal 80 residues or so.

Deletion mutants show that the fully structured region is limited to residues 243–319

In order to localize the sequential position of the random coil residues in the periplasmic domain of FtsN more precisely, a number of deletion mutants were cloned, overexpressed in ^{15}N-labelled form and then HSQC spectra recorded. Of the initial series of N-terminal deletions, only fragments 80–319 (ECN3) and 166–319 (ECN8) expressed in sufficient quantity to yield samples suitable for NMR. However, the HSQC spectra of these species quickly showed that a significant proportion of the random coil signals remained even in the shorter fragment. Closer inspection of the common sequences of those constructs revealed a region rich in glutamines, which was likely to be unfolded. Therefore, an internal deletion mutant was prepared (ECN9) that contained an N-terminal fragment (residues 58–128) and a C-terminal fragment (spanning residues 243–319) with a thrombin cleavage site in between. An HSQC spectrum of the uncleaved internal deletion mutant again showed quite a high proportion of random coil signals, so thrombin cleavage was used to separate the N-terminal (58–128) and C-terminal (243–319) parts of the fragment in order to allow these to be analysed separately. Heteronuclear single quantum correlation spectra of these two fragments are shown in Fig. 2C and D, respectively. It is immediately apparent that the C-terminal fragment corresponds to a well-folded domain with few if any random coil signals remaining (Fig. 2D). Furthermore, careful comparison of this spectrum with that from the complete periplasmic domain (Fig. 2B) showed that essentially all of the cross peaks in

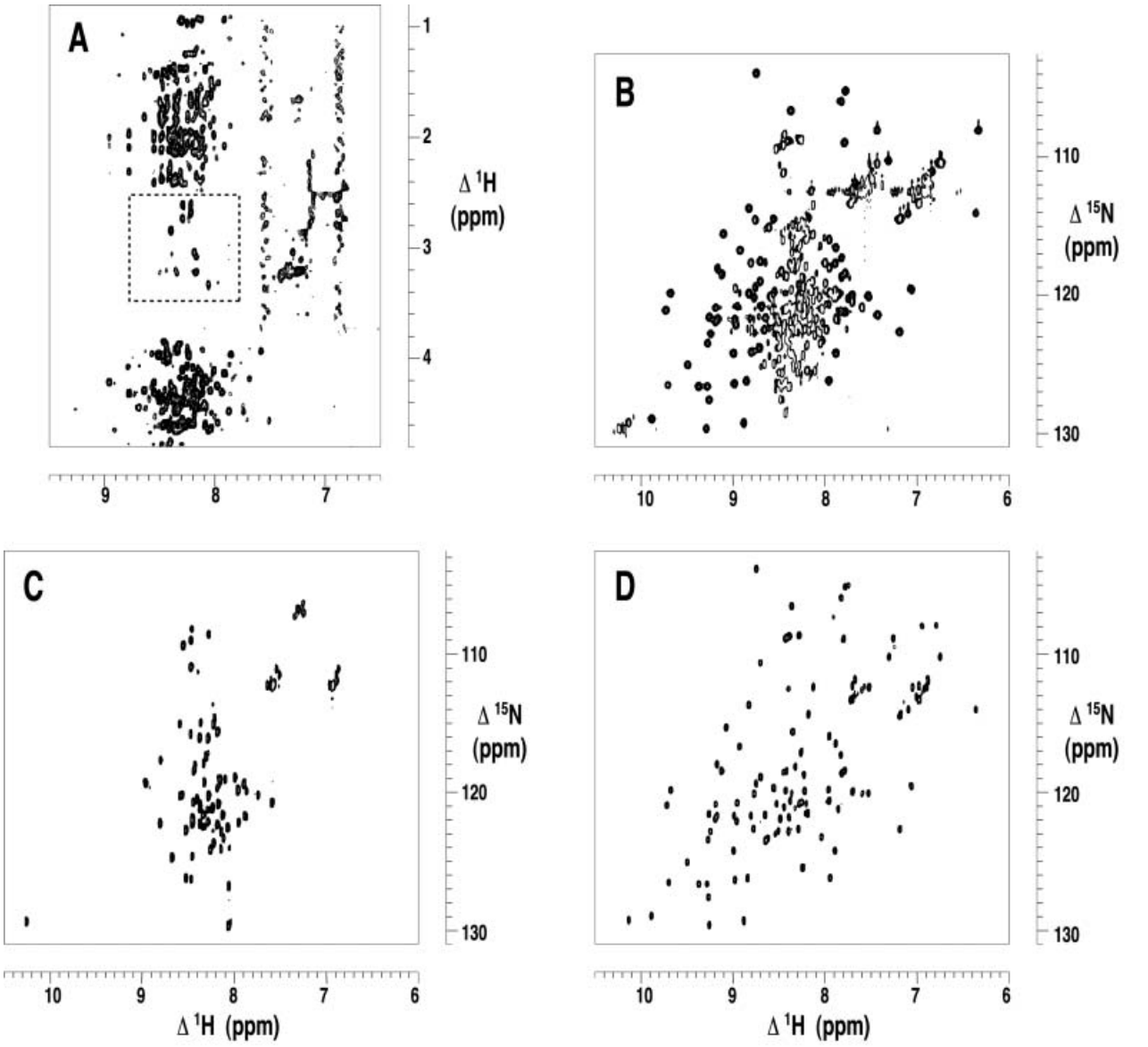

Fig. 2. NMR spectra of FtsN fragments.
A. Shows part of a homonuclear TOCSY spectrum of the complete periplasmic domain, FtsN 58–319. As TOCSY discriminates in favour of sharp signals, the strong cross-peaks seen here originate largely from the random coil region of this fragment. Only seven sets of cross-peaks are seen in the dashed box, which indicates the approximate expected region for (NH, H^{-}) cross peaks from random coil Asn, Asp, Cys, His, Phe, Tyr and Trp residues. This observation was very helpful in locating the random coil region of the sequence (see *Text*). Two vertical bands of artefacts (t_1-(t_1-noise) are visible at approx. 6.85 p.p.m. and 7.50 p.p.m.; these arise as a result of the very intense superimposed signals from the many side chain amide signals of Gln residues.
The remaining panels show HSQC spectra of ^{15}N-labelled samples of different FtsN fragments: (B) shows FtsN 58–319 (C) shows FtsN 58–128 and (D) shows FtsN 243–319. In (B) it can be seen that the spectrum of FtsN 58–319 comprises a mixture of signals from structured regions (well dispersed and somewhat broader signals) and random coil regions (poorly dispersed signals in the ^{1}H dimension, and somewhat sharper). In this presentation the random coil peaks, being sharper and therefore more intense, show up as having blank centres, because the contours plotted were chosen so as not to reach the tops of these peaks.
In (D) it can be seen that the C-terminal fragment 243–319 shows only well dispersed signals corresponding to a small structured domain. The absence of chemical shift differences for corresponding signals between panels (B) and (D) shows that this C-terminal structured domain does not interact with the remainder of the periplasmic domain, and that its structure is fully preserved in the shorter fragment. In (C) it can be seen that a small number of slightly dispersed signals are present, corresponding in part to the two short helices identified in this region of the sequence (see *Text*). As for the C-terminus, the near identity between corresponding shifts from this region in fragments 58–319 and 58–128 shows that these N-terminal helices do not interact with other regions of the periplasmic domain.

the HSQC spectrum of the 243–319 fragment have counterparts in the spectrum of the complete periplasmic domain, and that chemical shift differences between these corresponding peaks in the two spectra are absolutely minimal (dD_{max} = ~0.03 p.p.m.; for all but about five signals, dD_{max} = ~0 p.p.m). The fact that the resonances of the 243–319 fragment are, essentially, completely insensitive to the presence or absence of the remainder of the periplasmic domain provides very compelling evidence that: (i) the structure of this C-terminal fragment is unchanged by removal of residues 58–243, and (ii) the C-terminal structured domain does not interact to any measurable extent with any part of the remainder of the periplasmic domain.

Residues 243–319 of FtsN adopt an RNP-like fold

Given the relatively small size of this structured domain, and also the relatively low efficiency of incorporation of stable isotopes possible during preparation of NMR samples, we followed an NMR strategy based only on the use of natural abundance and ^{15}N-labelled protein samples. Nuclear magnetic resonances were assigned first to individual spin-systems (sets of resonances, each from within one amino-acid residue, linked through scalar couplings) using a combination of homonuclear TOCSY and heteronuclear 3D HSQC-TOCSY experiments. Spin-systems were then assembled onto the amino acid sequence using through-space connectivities measured in homonuclear NOESY and heteronuclear 3D HSQC-NOESY spectra, following the sequential assignment strategy developed by Wüthrich and co-workers (Wüthrich, 1986). Further analysis of these NOESY spectra generated assignments for the great majority of the remaining observed cross peaks, which were used to compile the constraint list for calculating the structure (see *Experimental procedures*). Notably, the fact that the cross peaks characteristic of folded structure observed in the NOESY spectrum of the complete periplasmic domain were essentially identical to those seen for the 243–319 fragment (data not shown) again provides strong evidence that the structure of the C-terminal fragment is unperturbed by the absence of the remainder of the periplasmic domain.

The structure computed by this process is shown in Figs 3 and 4. At an root mean square deviation (RMSD) of 0.62 Å (Table 1), the backbone precision of the structure is not especially high, but it is clearly more than sufficient to establish the detailed fold of the C-terminal domain with complete certainty. The domain adopts a βαββαβ topology, characteristic of a so-called 'RNP domain'. This name arises because early examples of the fold were mainly associated with RNA-binding proteins (Nagai *et al*., 1990), but subsequently it has become clear that this fold is extremely common, and is not associated with any particular function or even class of functions. A DALI search using the lowest energy structure from our NMR ensemble revealed a large number of close matches to proteins with a very diverse range of functions. For

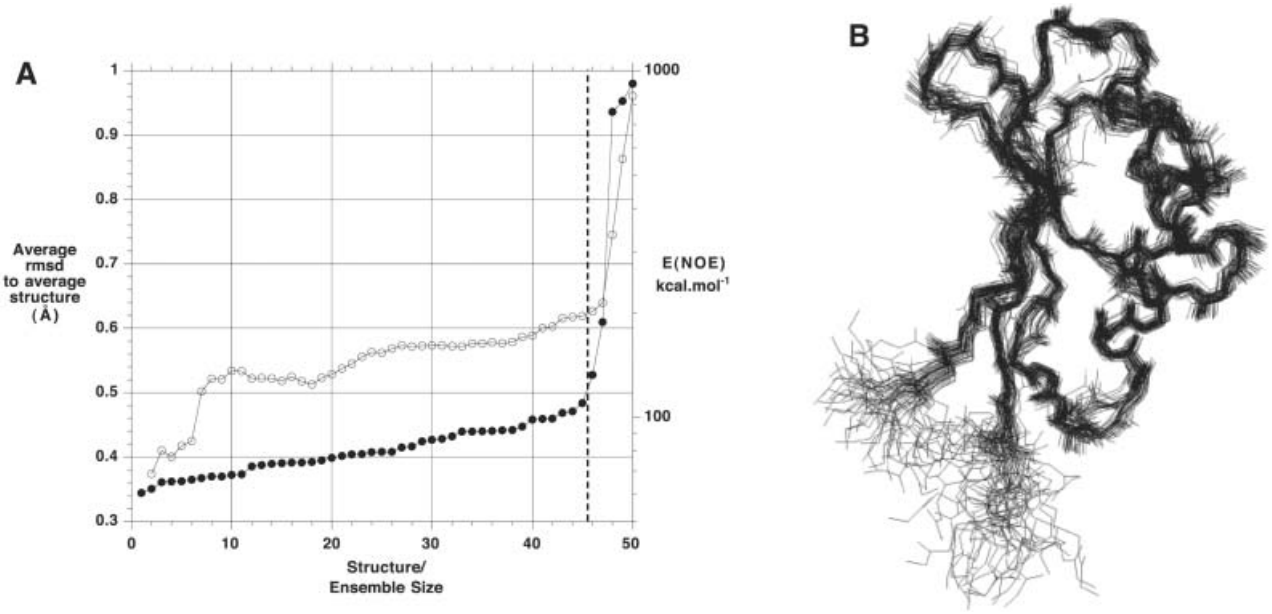

Fig. 3. A. RMSD and XPLOR NOE energy profiles (Fletcher *et al*., 1996) for the ensemble of calculated structures. The RMSD values (open circles) are independently calculated using each ensemble size, adding successive structures in order of increasing XPLOR NOE energy term. Filled circles represent the XPLOR energy terms. The vertical line after structure 45 indicates the end of the plateau region in these statistics, demonstrating the justification for discarding the last five structures from the ensemble used to calculate the structural statistics.
B. Superposition of the 45 accepted NMR structures in the final ensemble.

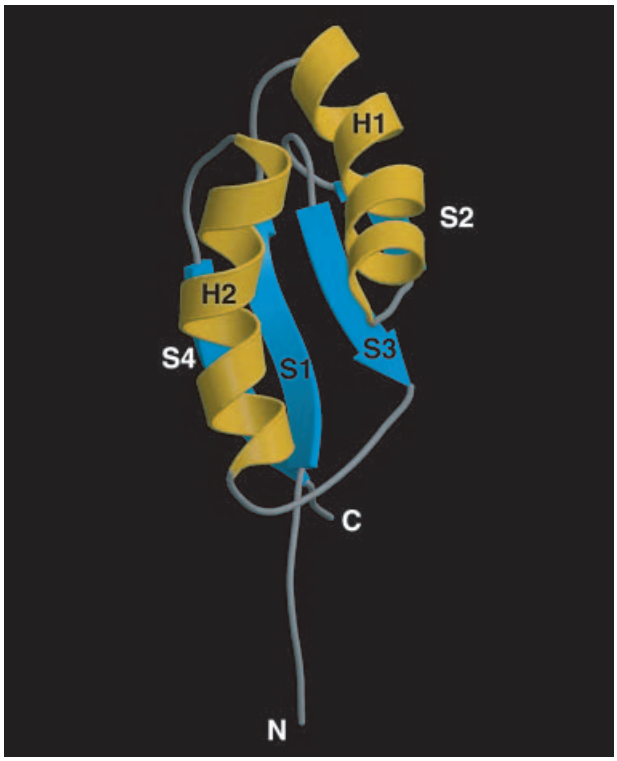

Fig. 4. Ribbon plot of the C-terminal domain of FtsN. The C-terminal 77 amino acids of FtsN adopt a βαββαβ topology, characteristic of a RNP domain. Secondary structure elements are labelled according to their appearance in the primary sequence of FtsN. The figure was prepared using the program MOLSCRIPT (Kraulis, 1991).

instance, the three highest scoring matches from this search were to a fragment of Porcine formiminotransferase-cyclodeaminase (Z = 5.7, RMSD = 2.8 Å, PDB code 1QD1), to *E. coli* signals transduction protein PII (Z = 5.5, RMSD = 2.3 Å, PDB code 2PII) and to HPV-18 E2 DNA-binding domain (Z = 5.4, RMSD = 2.5 Å, PDB code 1F9F).

Residues 58–128 of FtsN include three short helices

Analysis of the NMR spectra from FtsN 58–128 is significantly more difficult than for those of the structured C-terminal domain, because the signal dispersion is very much lower. Nevertheless, partial but unambiguous assignments were accessible, largely due to the unique occurrence of some residue types easily distinguishable by NMR (e.g. Tyr, Trp and Ile) and the infrequent occurrence of others (e.g. Ala and Val). The great majority ^{15}N and ^{1}H assignments were made for the backbone amide groups in this fragment, as well as a high proportion of the H^{-} and sidechain proton assignments (see *Supplementary material,* Table S1). Analysis of NOESY spectra of the 58–128 fragment showed about 25 weak sequential NH-NH cross peaks as well about 5 weak H^{-}(i) to NH(i + 3) cross peaks, both of which types of cross peak suggest the presence of helices. The assigned NOE cross peaks of these types are collected in *Supplementary material*, Table S2, and together they suggest that there may be at least some helical character in the regions (approximately) 62–67, 80–93 and 117–123. Although this analysis was not sufficiently rigorous to establish the precise boundaries of these helices with certainty, it is striking that they do correspond closely with the secondary structural predictions made by PHD (Profiling network prediction Heidelberg; http://www.embl-heidelberg.de/predictprotein/predictprotein.html). However, it is important to note that the NOE cross peaks are significantly weaker than would be expected for a well-ordered structure (e.g. those from the RNP domain in FtsN 243–319), and the signals from these regions are not noticeably less sharp than others in this predominantly unfolded fragment, suggesting that these putative helices are not fully formed. Furthermore, the fact that chemical shifts of signals from these partially helical regions in the 58–128 fragment are essentially identical to the corresponding shifts in the complete periplasmic domain 58–319 shows that these regions do not interact appreciably with the folded RNP domain.

Sequence comparison of FtsN 243–319 with an autolysin

A BLAST search with the structured domain of the C-terminus of FtsN revealed significant sequence homology (29% identity) to the autolysin CwlC (Fig. 5). CwlC is a sporulation-specific *N*-acteylmuramoyl-L-alanine amidase of *Bacillus subtilis*, the substrate-recognition domain of which is located at the C-terminus (Kuroda *et al.*, 1992; 1993). The remarkable sequence similarity between FtsN and the substrate-binding domain of this amidase will require an investigation into possible murein binding of the RNP domain of FtsN. Because of the hydrophilic nature of the substrate, no hydrophobic pocket is expected (and can be found) on the surface of the FtsN C-terminal RNP domain, guiding to a possible murein binding site.

FtsN contains five separate domains

As described above, the periplasmic part of FtsN can be divided into a region close to the membrane that partially folds into three helices that are not permanently arranged into a higher-order globular structure, a fairly extended, glutamine-rich, low complexity linker that has no detectable secondary structure and the C-terminal RNP domain. Together with the cytosolic 33 residues and the single *trans*-membrane helix this accounts for five structurally and potentially functionally distinct domains. The finding of low-complexity regions in pro-

```
FtsN S. flexneri     242 KKDERRWMVQ CGSFRGAEQA ETVRAQLAFE GFDSKITTNN GWNRVVIGPV KGKENADSTL NRLKMAGHTN CIRLAAGG 319
FtsN Y. pestis       204 KEKTQRWMVQ CGSFKAVDQA ESIRAQLAFA GIESRITSGG GWNRVVLGPY NSKAAADKAL QRLQGAGQSG CIPLSVGG 281
FtsN S. typhimurium  247 KKDERRWMVQ CGSFKGAEQA ESVRAQLAFE GFDSKITTNN GWNRVVIGPV KGKENADSTI NRLKMAGHTN CIRLATGG 324
FtsN E. coli         241 KKDERRWMVQ CGSFRGAEQA ETVRAQLAFE GFDSKITTNN GWNRVVIGPV KGKENADSTL NRLKMAGHTN CIRLAAGG 318
                                 : ||  |.|:    | :.. .    . |||| :   . |  :| ||     |:|||.    | | ||     : | .
CWLC B. subtilis     180 TSSSGLYKVQ IGAFKVKANA DSLASNAEAK GFDSIVLLKD GLYKVQIGAF SSKDNADTLA ARAKNAGFDA IVILES.. 255
```

Fig. 5. Alignment of FtsN C-terminal sequences with autolysin. The C-terminal domain of FtsN from *E. coli* has a sequence identity of 29% to the substrate recognition domain of the autolysin CWLC (*N*-acetylmuramoyl-L-alanine amidase) of *B. subtilis* (SWALL accession code: Q06320). Sequence alignment was made using 'GAP' and 'CLUSTALW' in the GCG-Wisconsin package (Genetics Computer Group, 1991).

teins is very common and many cytosolic and periplasmic proteins contain these segments, also in bacteria. What is maybe surprising is the size of the unstructured part of FtsN of about 180 residues if the three partially formed helices near the membrane are included. Disordered regions in proteins can have many functions, including protein–protein interactions and we believe this is most likely the case for the three helices that might interact with other proteins in the septal machinery, although there is currently no direct evidence for this. The helical part of the periplasmic domain of FtsN could bind to another protein and could then adopt a more ordered structure. This idea is supported by very high sequence conservation in this region when comparing FtsN sequences from a variety of organisms. The conservation is as high as in the C-terminal, RNP domain part (data not shown). We believe protein–protein interactions are unlikely for the glutamine-rich domain (residues 124–216). Both the cytosolic and *trans*-membrane part of FtsN are not essential for its function in cell division (Dai *et al*., 1996; Addinall *et al*., 1997)

A model for the function of FtsN

Genetic evidence suggested that FtsN is assembled late into the divisome when the murein shaping proteins FtsI (PBP3) and AmiC are also recruited. Localization of FtsN to the septum requires only the periplasmic part of the protein. From a structural point of view, an estimate of the size of the various subdomains of the periplasmic portion of FtsN (Fig. 6) shows that the long, flexible region connecting the *trans*-membrane helix and the RNP domain could easily allow the C-terminus of FtsN to reach over to the peptidoglycan layer. An estimate of the size of the periplasmic portion of FtsN certainly provides enough suppleness to reach the peptidoglycan layer. The RNP domain of FtsN, with its sequence similarity to murein-binding proteins does contribute to the specific recognition of glycan strands (W. Vollmer, pers. comm.), making it likely that FtsN functions in some way as a bridge, joining the divisome with the peptidoglycan layer. Once the divisome constricts the inner membrane, the connection with the peptidoglycan layer through FtsN ensures the constriction of the cell wall. This could theoretically be done by transmitting force from the septal ring to the cell wall or in opposite direction. Another possibility is the synchronization of events in the divisome and the murein layer by the interaction with cell wall modifying enzymes or other proteins in the divisome. Dai *et al*. (1996) have shown however, that the membrane anchor of FtsN can be functionally replaced with the cleavable signal sequence of MalE, possibly producing an non-membrane bound version of the periplasmic part of FtsN. If the cleavage reaction in this experiment takes a long time or is not 100% effective, functional FtsN molecules could still be bridging the periplasm, as localization is dependent only on specificity in the periplasmic part.

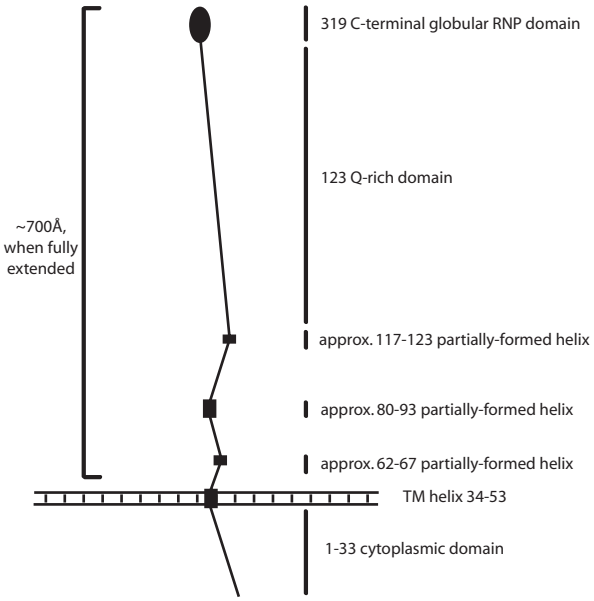

Fig. 6. Domain architecture of FtsN as analysed by sequential deletion mutagenesis and structural analyses by NMR. The globular C-terminal domain, which has the potential of interacting with the peptidoglycan layer, is connected via a long, glutamine (Q)-rich linker to three short, only partially formed helices that are anchored in the inner membrane by a *trans*-membrane (TM) helix. The indicated dimension reflects the maximum possible length the protein could adopt if the unfolded portion of the backbone were to adopt a fully extended conformation. In practice, the length would presumably be shorter as the unfolded portion of the chain would exchange between an ensemble of different conformations. Although the extent of such shortening is unknown, it still seems entirely plausible that the protein should have sufficient length to bridge the periplasmic space, the width of which is likely to be in the region of 130–250 Å (Oliver, 1996).

Table 1. Statistics relating to the final ensemble of structures of FtsN.

Structural restraints:	
Intra-residue	137
Sequential	176
Medium range ($2 \leq \|i-j\| \leq 4$)	78
Long range ($\|i-j\| > 4$)	163
Total	554 (=7.1 per residue)
Statistics for 45 accepted structures:	
Mean CNS energy term (kcal mol^{-1} ± SD)	
E(total)	320.6 ± 37.1
E(van der Waals)	102.5 ± 13.2
E(distance restraints)	80.5 ± 12.5
RMS deviations from the ideal geometry used within CNS	
Bond lengths	0.0035 Å
Bond angles	0.55°
Improper angles	0.50°
Average atomic RMS deviations from the average structure (±SD): (N, C^a, C atoms of both subunits simultaneously)	
Residues 5–75	0.62 ± 0.15 Å
(All heavy atoms)	
Residues 5–75	1.20 ± 0.17 Å

NOE-derived distance restraints	
Very strong (0–2.3 Å)	44
Strong (0–2.9 Å)	137
Medium (0–3.5 Å)	190
Weak (0–5.0 Å)	183

Experimental procedures

Cloning and purification of the complete periplasmic domain of FtsN

The gene encoding the periplasmic region (ECN2; residues 58–319) of FtsN (SWALL acc. nr. P29131) from *E. coli* was amplified by PCR using Pfu turbo polymerase (Stratagene) and the *Nde*I/*Bam*HI-digested fragment was cloned into pHis17. The protein was expressed under the control of the T7 promoter and has eight residues attached to the C-terminus (GSHHHHHH). The plasmids were transformed into C41(DE3) cells (Miroux and Walker, 1996) and the cells, grown in 2× TY, were induced with 1 mM isopropyl-β-D-thiogalactoside (IPTG) once the OD_{600} reached a value of 0.4. After 6 h the cells were harvested and frozen in liquid nitrogen. The protein was purified over a Ni^{2+}-NTA column as described previously (van den Ent and Löwe, 2000) and peak fractions were concentrated and further purified over a HiPrep 16/60 Sephacryl S200 column (Amersham) in 20 mM Na-Phosphate, pH 6.0, 1 mM EDTA, 1 mM DTT. The protein eluted as a single peak and could be stored for several months at 4°C.

Cloning and expression of deletion mutants of FtsN

The N-terminal deletion mutants of FtsN were cloned as described for the periplasmic region, with ECN3 containing amino acids 80–319 and ECN8 spanning residues 166–319. The internal deletion mutant, ECN9, was cloned as a *Nde*I/*Bam*HI fragment into pHis17 after the amplified 5′ end (encoding residues 58–128) and the 3′ end (encoding residues 243–319) were cleaved with *Spe*I and ligated. The linker between the N-terminal fragment and the C-terminal fragment contains a thrombin cleavage site (TSLVPRGS), where thrombin cleaves after the glycine. The proteins were purified essentially as described above. The N-terminal and C-terminal domains were separated by thrombin cleavage on the Ni^{2+}-NTA column for 16 h at room temperature. The N-terminal domain was collected in the flow through and the C-terminal fragment eluted with 300 mM imidazole. Both the N- and C-terminal domains were concentrated and further purified by gel filtration on a Superdex75 column (Amersham) in 20 mM Na-phosphate, pH 6.0, 1 mM EDTA, 1 mM DTT. The C-terminus of FtsN 243–319, for which structures were calculated, has the sequence 5'-KDERRWMV QCGSFRGAEQ AETVRAQLAF EGFDSKITTN NGWNRVVIGP VKGK ENADST LNRLKMAGHT NCIRLAAGG-3' (breaks are included for readability only, and occur immediately after residues 250, 260, 270, 280, 290, 300 and 310). The NMR samples contained, in addition, an N-terminal serine residue (from the thrombin cleavage site) and a C-terminal sequence GSHHHHHH (from the hexa-histidyl affinity tag).

^{15}N-labelled protein expression

A preculture, grown in 2× TY, was used in a 1:1000 dilution to inoculate 125 ml minimal medium containing 1× M9 without NH_4Cl supplemented with 0.4% glucose, 2 mM $MgSO_4$, 100 μg ml^{-1} ampicillin, 10 ng ml^{-1} $CaCl_2$, 0.6 g l^{-1} ^{15}N-NH_4Cl_2 (Sigma/Aldrich), 1 μg ml^{-1} of each of the vitamins (riboflavin, niacinamide, pyrodoxine, thiamine) and a 1:100 dilution of the trace elements (5 g Na_2EDTA, 0.8 g $FeCl_3.6H_2O$, 0.05 g $ZnCl_2$, 0.01 g $CuCl_2$, 0.01 g $CoCl_2.6H_2O$, 0.01 g H_2BO_3, 1.6 g $MnCl_2.4H_2O$, pH 7.0). The overnight culture was diluted 1:50 into 5 l minimal medium supplemented as described above and induced with 1 mM IPTG once the OD_{600} reached 0.4. After 6 h at 37°C the cells were harvested, frozen in liquid nitrogen and the proteins purified as described above.

NMR Spectroscopy

Nuclear magnetic resonance spectra were recorded on Bruker DMX 600, DRX 500 and Avance 800 spectrometers, each equipped with a 5 mm triple-resonance (^{1}H/^{15}N/^{13}C)

single-axis gradient probe. Data were processed using the program XWIN-NMR (Bruker GmbH, Karlsruhe, Germany) and analysed using the programs XWIN-NMR and SPARKY (Goddard). Homonuclear experiments included 2D (^{1}H, ^{1}H) NOESY, TOCSY and correlation spectroscopy (COSY) experiments (spectral widths of 8 kHz in both dimensions, and using selective irradiation during the relaxation delay to suppress the water signal). TOCSY experiments employed the DIPSI-2 mixing sequence (Shaka *et al*., 1988). with a spin-lock field strength of 4.5 kHz and a mixing time of 57 ms (corresponding to nine complete cycles of DIPSI-2). Heteronuclear experiments included 2D ^{15}N-HSQC, 3D ^{15}N NOESY-HSQC, 3D ^{15}N TOCSY-HSQC and 3D ^{15}N-HSQC-NOESY-HSQC. In all of the above experiments, spectral widths were generally 7–8 kHz for protons and 1.0–1.1 kHz for ^{15}N. Mixing times for 2D ^{1}H, ^{1}H NOESY were 50, 100 and 150 ms, and for 3D ^{15}N NOESY experiments 150 ms. All spectra were acquired in phase-sensitive mode and frequency discrimination in indirect dimensions was achieved using either time-proportional phase incrementation (TPPI), States-TPPI or echo-antiecho (for ^{15}N dimensions with gradient selection). Water suppression was achieved by selective irradiation during the relaxation delay and during the mixing time in NOESY and HSQC-NOESY experiments. ^{1}H and ^{15}N chemical shifts were referenced following the method described by Wishart *et al*. (1995) using sodium 3,3,3–trimethylsilylpropionate (TSP) as internal ^{1}H reference. An essentially complete assignment of the ^{1}H and ^{15}N resonances was achieved using the sequential assignment NOE-based approach (Wüthrich, 1986).

Structural calculations

Nuclear Overhauser effect intensities were measured in 2D NOESY and 3D ^{15}N-NOESY-HSQC spectra at mixing times of 50 ms, 100 ms and 150 ms. Cross peaks were categorized in 2D NOESY spectra using sequential $d_{\alpha N}$(i, i +1) connectivities from within β-strands to define the upper bound of the category 'very strong' (0–2.3 Å), sequential d_{NN}(i, i +1) connectivities from within helices to define the upper bound of the category 'strong' (0–2.9 Å), and $d_{\alpha N}$(i, i +3) connectivities from within helices to define the upper bound for the category 'medium' (0–3.5 Å). Remaining peaks were classified as 'weak' (0–5.0 Å). Lower bounds for all NOE restraints were set to 0.0 Å (Hommel *et al*., 1992). No multiplicity corrections for restraints involving genuinely equivalent spins were needed, as $< r^{-6} >$ summation was used during the structure calculation protocol.

Structures were calculated from polypeptide chains with randomized *f* and *y* torsion angles using the simulated annealing protocol supplied with the program CNS. Calculations employed torsional dynamics at 50 000 K for 1000 steps of 15 ps, then a first slow cooling stage of torsional dynamics (200 cycles each of 1000 steps of 15 ps, decreasing the temperature by 250K per cycle from 50 000 K to 0 K), a second slow cooling stage of Cartesian dynamics (80 cycles each of 3000 steps of 15 ps, decreasing the temperature by 25 K per cycle from 2 000 K to 0 K), and finally 2000 steps of Powell minimization. In all structure calculations, the force field comprised only geometric terms (bond lengths and angles, van der Waals repulsive terms and restraints to maintain correct chirality for chiral centres, planarity for peptide bonds and aromatic rings); electrostatic, van der Waals attractive and generalized hydrogen bonding terms were not included. Randomly different starting velocities were used for each of 50 structure calculations, and the 45 converged structures that were accepted corresponded to a plateau in both the energy-ordered rmsd profile and in the NOE energy itself (Fig. 3). The program CLUSTERPOSE (Diamond, 1992; 1995) was used to calculate average structures of ensembles of NMR structures and determine the mean rmsd of these ensembles to the mean structure (Table 1).

Data deposition

^{1}H and ^{15}N NMR resonance assignments for FtsN at 27°C and pH 6.5 have been deposited in the BioMagResBank (BMRB) with accession code 5984. Atomic coordinates for the ensemble of 45 final structures (calculated including hydrogen bond restraints) of FtsN have been deposited in the Protein Data Bank (PDB) with accession code 1UTA.

Supplementary material

The following material is available from
http://www.blackwellpublishing.com/products/journals/suppmat/mmi/mmi3991/mmi3991sm.htm

Table S1. Partial assignments for the 58–128 fragment of FtsN. Residues M57 and T129-G135 (italicized in the Table) arise from the construct and are non-native, but are numbered sequentially here for ease of reference.

Table S2. NOE cross peaks consistent with the proposed weakly helical regions (E62-S67, E80-Q93 and E117-E123) referred to in the paper. Residues M57 and T129-G135 arise from the construct and are non-native, but are numbered sequentially here for ease of reference. Residues A127-L132 apparently contribute a fourth helix, the Table entries for which are italicized here because they involve non-native residues.

References

Adam, M., Fraipont, C., Rhazi, N., NguyenDisteche, M., Lakaye, B., Frere, J.M., *et al.* (1997) The bimodular G57–V577 polypeptide chain of the class B penicillin-binding protein 3 of *Escherichia coli* catalyzes peptide bond formation from thiolesters and does not catalyze glycan chain polymerization from the lipid II intermediate. *J Bacteriol* **179:** 6005–6009.

Addinall, S.G., Cao, C., and Lutkenhaus, J. (1997) FtsN, a late recruit to the septum in *Escherichia coli*. *Mol Microbiol* **25:** 303–309.

Bernhardt, T.G., and de Boer, P.A.J. (2003) The *Escherichia coli* amidase AmiC is a periplasmic septal ring component exported via the twin-arginine transport pathway. *Mol Microbiol* **48:** 1171–1182.

Dai, K., Xu, Y.F., and Lutkenhaus, J. (1993) Cloning and characterization of *ftsn*, an essential cell-division gene in *Escherichia coli* isolated as a multicopy suppressor of *ftsn*12 (Ts). *J Bacteriol* **175:** 3790–3797.

Dai, K., Xu, Y.F., and Lutkenhaus, J. (1996) Topological characterization of the essential *Escherichia coli* cell division protein FtsN. *J Bacteriol* **178:** 1328–1334.

Diamond, R. (1992) On the multiple simultaneous superposition of molecular-structures by rigid body transformations. *Protein Sci* **1:** 1279–1287.

Diamond, R. (1995) Coordinate-based cluster-analysis. *Acta Crystallogr Section D-Biol Crystallogr* **51:** 127–135.

Draper, G.C., McLennan, N., Begg, K., Masters, M., and Donachie, W.D. (1998) Only the C-terminal domain of FtsK functions in cell division. *J Bacteriol* **180:** 4621–4627.

van den Ent, F., and Löwe, J. (2000) Crystal structure of the cell division protein FtsA from *Thermotoga maritima*. *EMBO J* **19:** 5300–5307.

Errington, J., Daniel, R.A., and Scheffers, D.J. (2003) Cytokinesis in bacteria. *Microbiol Mol Biol Rev* **67:** 52–65.

Fletcher, C.M., Jones, D.N.M., Diamond, R., and Neuhaus, D. (1996) Treatment of NOE constraints involving equivalent or nonstereoassigned protons in calculations of biomacromolecular structures. *J Biomolecular Nmr* **8:** 292–310.

Genetics Computer Group (1991*) Program Manual for the GCG Package.* Wisconsin.

Goddard, T.D., and Kneller, D.G. () SPARKY. 3. San Fransisco: Univeristy of California.

Heidrich, C., Templin, M.F., Ursinus, A., Merdanovic, M., Berger, J., Schwarz, H., *et al.* (2001) Involvement of N-acetylmuramyl-L-alanine amidases in cell separation and antibiotic-induced autolysis of *Escherichia coli*. *Mol Microbiol* **41:** 167–178.

Heidrich, C., Ursinus, A., Berger, J., Schwarz, H., and Holtje, J.V. (2002) Effects of multiple deletions of murein hydrolases on viability, septum cleavage, and sensitivity to large toxic molecules in *Escherichia coli*. *J Bacteriol* **184:** 6093–6099.

Hommel, U., Harvey, T.S., Driscoll, P.C., and Campbell, I.D. (1992) Human epidermal growth-factor – high-resolution solution structure and comparison with human transforming growth factor-alpha. *J Mol Biol* **227:** 271–282.

Ishino, F., and Matsuhashi, M. (1981) Peptidoglycan synthetic enzyme-activities of highly purified penicillin-binding protein-3 in *Escherichia coli* – a septum-forming reaction sequence. *Biochem Biophys Res Comms* **101:** 905–911.

Kraulis, P.J. (1991) MOLSCRIPT: a program to produce both detailed and schematic plots of protein structures. *J Appl Crystallogr* **24:** 946–950.

Kuroda, A., Asami, Y., and Sekiguchi, J. (1993) Molecular-cloning of a sporulation-specific cell-wall hydrolase gene of *Bacillus subtilis*. *J Bacteriol* **175:** 6260–6268.

Kuroda, A., Sugimoto, Y., Funahashi, T., and Sekiguchi, J. (1992) Genetic-structure, isolation and characterization of a *Bacillus licheniformis* cell-wall hydrolase. *Mol Gen Genet* **234:** 129–137.

Lutkenhaus, J., and Addinall, S.G. (1997) Bacterial cell division and the Z ring. *Annu Rev Biochem* **66:** 93–116.

Miroux, B., and Walker, J.E. (1996) Over-production of proteins in *Escherichia coli*: mutant hosts that allow synthesis of some membrane proteins and globular proteins at high levels. *J Mol Biol* **260:** 289–298.

Nagai, K., Oubridge, C., Jessen, T.H., Li, J., and Evans, P.R. (1990) Crystal-structure of the RNA-binding domain of the U1 small nuclear ribonucleoprotein-A. *Nature* **348:** 515–520.

Oliver, D.B. (1996) Periplasm. In *Escherichia Coli and Salmonella*, Vol. 1. Neidhardt, F.D. (ed.). Washington: American Society for Microbiology Press, pp. 88–104.

Rothfield, L., Justice, S., and GarciaLara, J. (1999) Bacterial cell division. *Annu Rev Genet* **33:** 423–448.

Shaka, A.J., Lee, C.J., and Pines, A. (1988) Iterative schemes for bilinear operators – application to spin decoupling. *J Magnetic Resonance* **77:** 274–293.

Vollmer, W., and Holtje, J.V. (2001) Morphogenesis of *Escherichia coli*. *Current Opinion Microbiol* **4:** 625–633.

Wishart, D.S., Bigam, C.G., Yao, J., Abildgaard, F., Dyson, H.J., Oldfield, E., *et al.* (1995) H-1, C-13 and N-15 chemical-shift referencing in biomolecular NMR. *J Biomolecular NMR* **6:** 135–140.

Wüthrich, K. (1986) *NMR of Proteins and Nucleic Acids*. New York: John Wiley.